ANL/NDM--71

DE82 019475

ANL/NDM-71

FAST-NEUTRON TOTAL AND SCATTERING CROSS SECTIONS OF ELEMENTAL PALLADIUM[*]

by

A. B. Smith, P. T. Guenther and J. F. Whalen

June 1982

Applied Physics Division
Argonne National Laboratory
9700 South Cass Avenue
Argonne, Illinois 60439
USA

OTHER ISSUES IN THE ANL/NDM SERIES ARE:

ANL/NDM-1   Cobalt Fast Neutron Cross Sections-Measurement and Evaluation by
             P. T. Guenther, P. A. Moldauer, A. B. Smith, D. L. Smith and J.
             F. Whalen, July 1973.

ANL/NDM-2   Prompt Air-Scattering Corrections for a Fast-Neutron Fission
             Detector: $E_n \leq 5$ MeV by Donald L. Smith, September 1973.

ANL/NDM-3   Neutron Scattering from Titanium; Compound and Direct Effects
             by E. Barnard, J. deVilliers, P. Moldauer, D. Reitmann, A. Smith
             and J. Whalen, October 1973.

ANL/NDM-4 ^{90}Zr and ^{92}Zr; Neutron Total and Scattering Cross Sections by
             P. Guenther, A. Smith and J. Whalen, July 1974.

ANL/NDM-5   Delayed Neutron Data - Review and Evaluation by Samson A. Cox,
             April 1974.

ANL/NDM-6   Evaluated Neutronic Cross Section File for Niobium by R. Howerton,
             Lawrence Livermore Laboratory and A. Smith, P. Guenther and J.
             Whalen, Argonne National Laboratory, May 1974.

ANL/NDM-7   Neutron Total and Scattering Cross Sections of Some Even Isotopes
             of Molybdenum and the Optical Model by A. B. Smith, P. T. Guenther
             and J. F. Whalen, June 1974.

ANL/NDM-8   Fast Neutron Capture and Activation Cross Sections of Niobium
             Isotopes by W. P. Poenitz, May 1974.

ANL/NDM-9   Method of Neutron Activation Cross Section Measurement for $E_n =$
             5.5-10 MeV Using the D(d,n)He-3 Reaction as a Neutron Source by
             D. L. Smith and J. W. Meadows, August 1974.

ANL/NDM-10   Cross Sections for (n,p) Reactions on ^{27}Al, ^{46,47,48}Ti, ^{54,56}Fe,
             ^{58}Ni, ^{59}Co and ^{64}Zn from Near Threshold to 10 MeV by Donald L.
             Smith and James W. Meadows, January 1975.

ANL/NDM-11   Measured and Evaluated Fast Neutron Cross Sections of Elemental
             Nickel by P. Guenther, A. Smith, D. Smith and J. Whalen, Argonne
             National Laboratory and R. Howerton, Lawrence Livermore Laboratory,
             July 1975.

ANL/NDM-12   A Spectrometer for the Investigation of Gamma Radiation Produced
             by Neutron-Induced Reactions by Donald L. Smith, April 1975.

ANL/NDM-13   Response of Several Threshold Reactions in Reference Fission
             Neutron Fields by Donald L. Smith and James W. Meadows, June 1975.

ANL/NDM-14   Cross Sections for the ^{66}Zn(n,p)^{66}Cu, ^{113}In(n,n')^{113m}In and
             ^{115}In(n,n')^{115m}In Reactions from Near Threshold to 10 MeV by
             Donald L. Smith and James W. Meadows, July 1975.

ANL/NDM-46 Fast-Neutron Total and Scattering Cross Sections of ^{107}Ag in the MeV Region by A. Smith, P. Guenther, G. Winkler and J. Whalen, January 1979.

ANL/NDM-47 Scattering of MeV Neutrons from Elemental Iron by A. Smith and P. Guenther, March 1979.

ANL/NDM-48 ^{235}U Fission Mass and Counting Comparison and Standardization by W. P. Poenitz, J. W. Meadows and R. J. Armani, May 1979.

ANL/NDM-49 Some Comments on Resolution and the Analysis and Interpretation of Experimental Results from Differential Neutron Measurements by Donald L. Smith, November 1979.

ANL/NDM-50 Prompt-Fission-Neutron Spectra of ^{233}U, ^{235}U, ^{239}Pu and ^{240}Pu Relative to that of ^{252}Cf by A. Smith, P. Guenther, G. Winkler and R. McKnight, September 1979.

ANL/NDM-51 Measured and Evaluated Neutron Cross Sections of Elemental Bismuth by A. Smith, P. Guenther, D. Smith and J. Whalen, April 1980.

ANL/NDM-52 Neutron Total and Scattering Cross Sections of ^{6}Li in the Few MeV Region by P. Guenther, A. Smith and J. Whalen, February 1980.

ANL/NDM-53 Neutron Source Investigations in Support of the Cross Section Program at the Argonne Fast-Neutron Generator by James W. Meadows and Donald L. Smith, May 1980.

ANL/NDM-54 The Nonelastic-Scattering Cross Sections of Elemental Nickel by A. B. Smith, P. T. Guenther and J. F. Whalen, June 1980.

ANL/NDM-55 Thermal Neutron Calibration of a Tritium Extraction Facility using the ^{6}Li(n,t)^{4}He/^{197}Au(n,γ)^{198}Au Cross Section Ratio for Standardization by M. M. Bretscher and D. L. Smith, August 1980.

ANL/NDM-56 Fast-Neutron Interactions with ^{182}W, ^{184}W and ^{186}W by P. T. Guenther, A. B. Smith and J. F. Whalen, December 1980.

ANL/NDM-57 The Total, Elastic- and Inelastic-Scattering Fast-Neutron Cross Sections of Natural Chromium, Peter T. Guenther, Alan B. Smith and James F. Whalen, January 1981.

ANL/NDM-58 Review of Measurement Techniques for the Neutron Capture Process by W. P. Poenitz, August 1981.

ANL/NDM-59 Review of the Importance of the Neutron Capture Process in Fission Reactors, Wolfgang P. Poenitz, July 1981.

ANL/NDM-60 Neutron Capture Activation Cross Sections of ^{94}Zr, ^{96}Zr, ^{98,100}Mo, and ^{110,114,116}Cd at Thermal and 30 keV Energy, John M. Wyrick and Wolfgang P. Poenitz, (to be published).

ANL/NDM-61   Fast-neutron Total and Scattering Cross Sections of ^{58}Ni by
              Carl Budtz-Jørgensen, Peter T. Guenther, Alan B. Smith and
              James F. Whalen, September 1981.

ANL/NDM-62   Covariance Matrices and Applications to the Field of Nuclear
              Data, by Donald L. Smith, November 1981.

ANL/NDM-63   On Neutron Inelastic-Scattering Cross Sections of ^{232}Th, ^{233}U,
              ^{235}U, ^{238}U, ^{239}U, and ^{239}Pu and ^{240}Pu by Alan B. Smith and
              Peter T. Guenther, January 1982.

ANL/NDM-64   The Fission Fragment Angular Distributions and Total Kinetic
              Energies for ^{235}U(n,f) from .18 to 8.83 MeV by James W. Meadows,
              and Carl Budtz-Jørgensen, (to be published).

ANL/NDM-65   Note on the Elastic Scattering of Several MeV Neutrons from
              Elemental Calcium by Alan B. Smith and Peter T. Guenther
              (to be published).

ANL/NDM-66   Fast-neutron Scattering Cross Sections of Elemental Silver
              by Alan B. Smith and Peter T. Guenther (to be published).

ANL/NDM-67   Non-evaluation Applications for Covariance Matrices by
              Donand L. Smith, (to be published).

ANL/NDM-68   Fast-neutron Total and Scattering Cross Sections of ^{103}Rh
              by Alan B. Smith, Peter T. Guenther and James F. Whalen (to be
              published).

ANL/NDM-69   Fast-neutron Scattering Cross Sections of Elemental
              Zirconium by Alan B. Smith and Peter T. Guenther (to be
              published).

ANL/NDM-70   Fast-neutron Total and Scattering Cross Sections of Niobium
              by Alan B. Smith, Peter T. Guenther and James F. Whalen (to be
              published).

TABLE OF CONTENTS

Page

FAST-NEUTRON TOTAL AND SCATTERING
CROSS SECTIONS OF ELEMENTAL PALLADIUM[*]

by

A. B. Smith, P. T. Guenther and J. F. Whalen[*]
Argonne National Laboratory
Argonne, Illinois   60439

ABSTRACT

Neutron total cross sections of palladium are measured from
$\approx$ 0.6 to 4.5 MeV with resolutions of $\approx$ 30 to 70 keV at intervals
of $\leq$ 50 keV. Differential neutron elastic- and inelastic-scattering
cross sections are measured from 1.4 to 3.85 MeV at intervals of 50
to 100 keV and at 10 to 20 scattering angles distributed between $\approx$ 20
and 160 deg. The experimental results are compared with respective
quantities given in ENDF/B-V and used to deduce an optical potential
that provides a good description of the measured values.

I. INTRODUCTION

This work is a part of a continuing program of the experimental study of the interaction of fast-neutrons with fission-product nuclei. Elemental palladium consists of six isotopes. Five of them (^{102}Pd(1%), ^{104}Pd(11%), ^{106}Pd(27%), ^{108}Pd(27%) and ^{110}Pd(12%)) are even nuclei. The sixth isotope is the odd ^{105}Pd(22%). All of these isotopes occur in fission-product chains with high yields in cases of applied interest. For example, in the case of ^{239}Pu fission induced by fission-neutrons, the yields are 6.8% (^{104}Pd), 5.8% (^{105}Pd), 4.7% (^{106}Pd), 2.7% (^{108}Pd), and 0.9% (^{110}Pd). The characteristics of the low-lying levels of the even palladium isotopes suggest vibrational nuclei.[1] However, at the relatively low energies of the present experiments direct-vibrational excitations should not be strong and thus it is reasonable to describe the neutron interaction with a spherical optical model (OM) which can be subsequently used to calculate, particularly, the capture cross sections of the individual palladium isotopes.

Subsequent portions of this report; very briefly outline the experimental procedures (Sec. II), present the experimental results (Sec. III), discuss the derivation of an OM from the measured values (Sec. IV), and compare the experimental values with relevant quantities given in ENDF/B-V[2].

II. EXPERIMENTAL PROCEDURES

The experimental procedures used in the present neutron total- and scattering-cross-section measurements have been widely employed at the Argonne Fast-Neutron Generator. The details are given in the cited references and thus the following remarks are confined to a brief outline of the experimental procedures.

Both the neutron total- and scattering-cross-section measurements employed a 2 cm diameter 2 cm long cylinderical sample of elemental palladium metal. Sample density was determined from precision weight and dimension measurements to better than 0.1%. Chemical impurities in the sample were negligible.

Neutron total cross sections were deduced from the observed transmission of nonenergetic neutrons through the sample in the conventional manner.[3] The sample was arranged to alternate in the neutron beam with a void and carbon-reference sample with a frequency of $\approx$ 1 Hz. This rapid sample interchange made monitoring of the source intensity unnecessary. The neutron source was the ^{7}Li(p;n)^{7}Be reaction with the lithium thickness adjusted to give the desired incident-neutron energy spread. The source was pulsed on for durations of $\approx$ 1 nsec. Time-of-flight techniques were employed to select the primary neutron group from the source reaction and to surpress backgrounds. In-scattering corrections were negligible and a clock system assured proper correction for dead-time effects. The measurement-system fidelity was continually verified by the concurrent measurement of the well-known neutron total cross sections of carbon.[4] Details of the apparatus and its application are given in Ref. 5.

Neutron differential-scattering cross sections were measured using the Argonne ten-angle time-of-flight apparatus.[6] Again, the neutron source was the $^7Li(p;n)^7Be$ reaction pulsed on for durations of ≈ 1 nsec. Scattered neutron flight paths were ≈ 5.4 m. An additional time-of-flight system monitored the source intensity. The relative energy-dependent responses of the neutron detectors were determined by the observation of neutrons emitted at the spontaneous fission of ^{252}Cf.[7] The absolute response of the detector system was determined relative to the well-known neutron total cross sections of carbon[4] in the manner described in Ref. 8. This procedure yields palladium scattering cross sections relative to the neutron total cross section of carbon. All of the scattering results were corrected for multiple-event, beam-attenuation, and angular-resolution effects using the procedures of Ref. 9. Details of the scattering apparatus and its application are found in Refs. 6, 9 and 10.

III. EXPERIMENTAL RESULTS

A. Neutron Total Cross Sections

The neutron total cross sections were measured from ≈ 0.6 to 4.5 MeV at intervals of < 50 keV with incident-neutron energy spreads of ≈ 30 to 70 keV. The measured energy range was traversed several times. The experimental results were combined and averaged over 50 keV bins to obtain the results shown in Fig. 1. The statistical uncertainty of each individual datum is $\lesssim 1\%$ and the results are consistent to well within the experimental uncertainties. Self-shielding effects are not a factor at the energies of the present measurements.[5] The averaged values follow a smooth energy dependence with no indication of residual fluctuations.

The present neutron-total-cross-section results are in good agreement with the low-energy values of Lambropoulos et al.[11] and with the high-energy results of Foster and Glasgow.[12] There is excellent agreement with the recent results of Poenitz et al.[5] over the entire energy range of the present measurements as, illustrated in Fig. 1.

B. Neutron Elastic-Scattering Cross Sections

The elastic-scattering measurements were made at incident-neutron energy intervals of 50 to 100 keV from 1.4 to 3.85 MeV with incident-neutron energy spreads of 30 to 70 keV. Ten to twenty differential values were obtained at each incident energy, distributed between 20 and 160 deg. The scattered-neutron resolutions were sufficient to resolve the elastic-scattered component from all known inelastic-scattered contributions. The measured values were averaged over 200-keV energy increments using a running-average procedure in order to obtain an improved definition of the energy-averaged behavior. These averaged results are shown in Fig. 2. They follow a smooth energy dependence with no apparent residual fluctuations. The statistical uncertainties of the
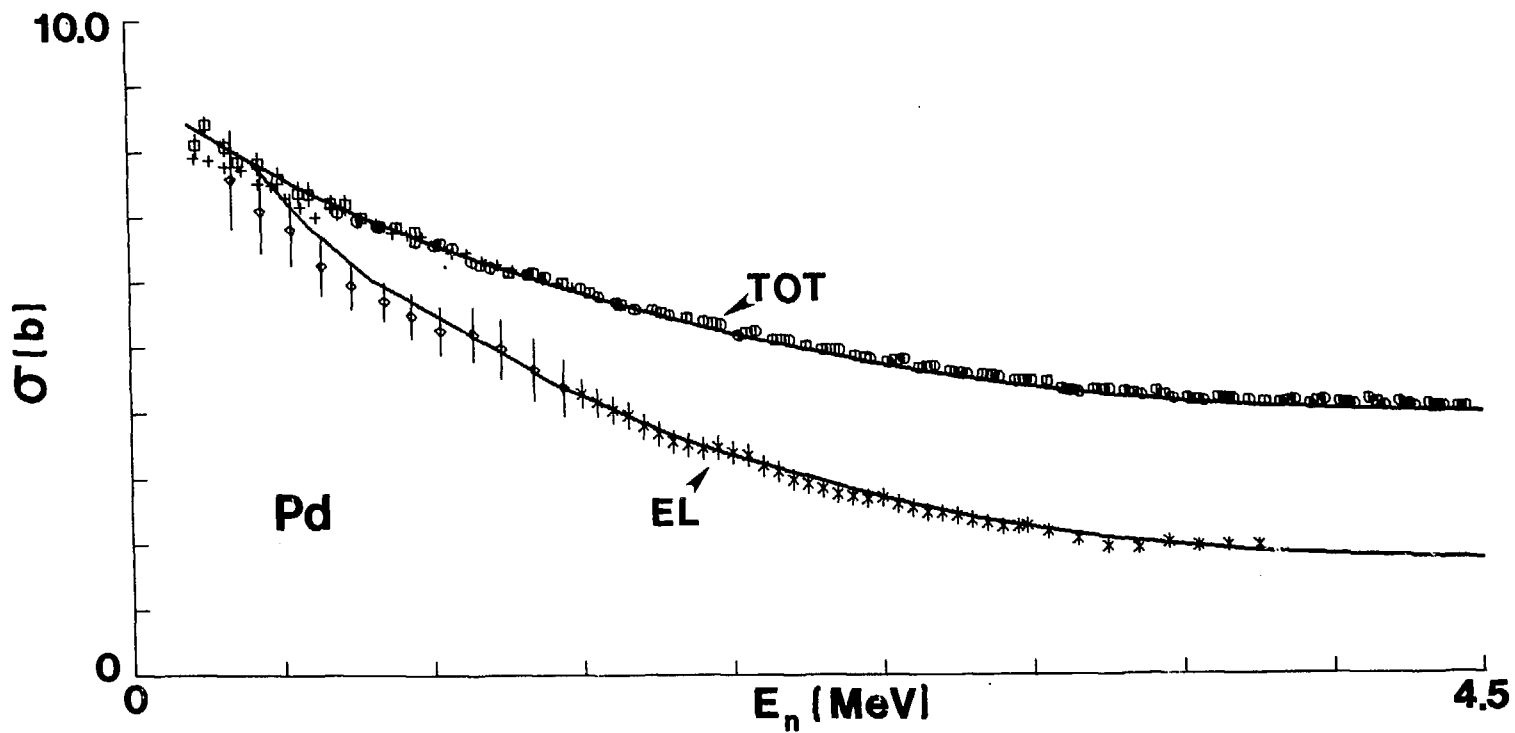
Fig. 1 Neutron Total and Elastic-Scattering Cross Sections of Palladium.
The present experimental results are indicated by 0 (totals) and
X (elastic scattering). Previously reported experimental values
are noted by; ▢ (totals of Ref. 5), + (totals of Ref. 11), and ◇
(elastics of Ref. 11). Curves are the results of model calcula-
tions as described in the text.

averaged differential values were $\leq$ 3% and frequently < 1%. Systematic uncertainties associated with the detector calibrations were $\leq$ 3% and calibrations were reproducible to within that uncertainty. The neutron-scattering angles were known to $\approx$ 3/4 deg. Correction procedures introduced an additional $\leq$ 1% uncertainty. Thus the overall uncertainties of the energy-averaged differential values were $\leq$ 5%. A region of exception is the extreme minima of the higher-energy distributions where the uncertainties can be larger.

The measured differential values were least-squares fitted with a 6th-order Legendre-polynomial series with the results shown in Fig. 2. The fitting procedures also provided the angle-integrated elastic scattering cross sections shown in Fig. 1. The estimated uncertainty of the latter is $\leq$ 5%. The present experimental results are in good agreement with the lower-energy values of Ref. 11 both with respect to the angle-integrated cross-section values (shown in Fig. 1) and the differential distributions.

C. Neutron Inelastic-Scattering Cross Sections

The average spacing of levels in elemental palladium to excitations of 1 MeV is $\leq$ 30 keV.[1] Resolution of such complex structure using time-of-flight techniques is formidable. The present measurements were further complicated by the second neutron group from the $^7Li(p;n)^7Be^*$ source reaction and by the intentionally relatively-broad incident-energy spreads. As a consequence, all of the inelastic-scattering results were "observed" excitations due to contributions from several reported levels[1] in the same or different isotopes.

The inelastic- and elastic-scattering measurements were made concurrently using the same scattering angles, incident energies and incident-energy resolutions. Excitation energies were accepted when observed with reasonable consistency at several scattering angles and incident energies. Ten firmly- and four tentatively-identified excitations were established as outlined in Table 1. The respective uncertainties are defined as the RMS deviations from the simple average of a number of measurements. These uncertainties should not be confused with scattered-neutron resolutions which were often larger due to instrument resolution and the character of the underlying level structure. The observed excitations can be correlated with reported levels in the five palladium isotopes[1] as suggested by the isotopic notation of Table 1.

Angle-integrated inelastic-scattering cross sections were derived from the differential measured values by fitting a low-order Legendre-polynomial series (P_n, with orders $n \leq 2$) to the observed quantities in a manner analogous to that employed above for elastic scattering. Most of the differential inelastic distributions were nearly isotropic. Corrections for the second neutron group from the source reaction were made where required. In some instances these corrections were speculative due to level and resolution uncertainties. The uncertainties attributed to the angle-integrated inelastic-scattering cross
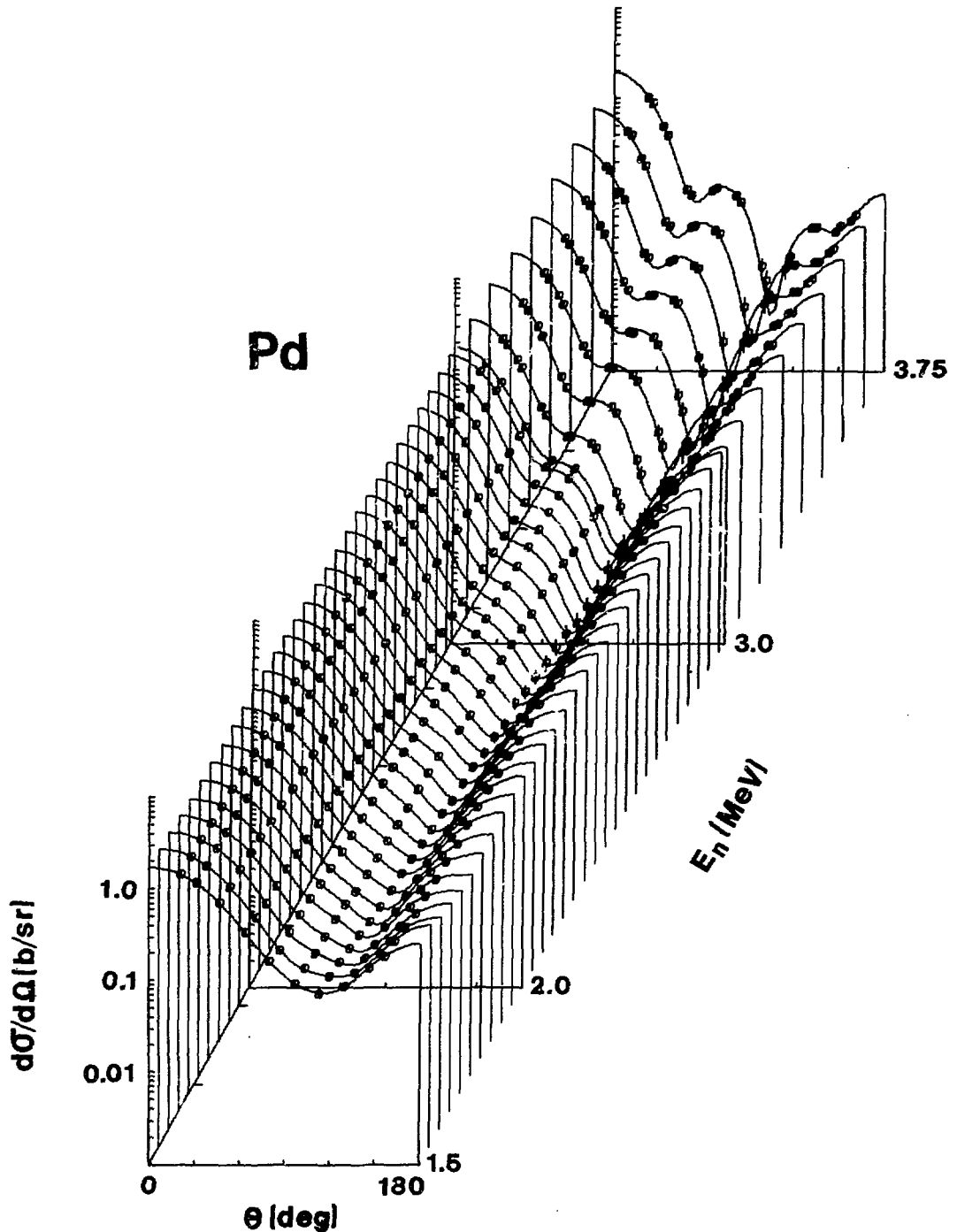
Fig. 2 Differential Elastic-Scattering Cross Sections of Elemental
Palladium. The present experimental results, averaged over a
200-keV incident-energy interval, are indicated by data symbols.
Curves denote the results of fitting the measured values with
Legendre-polynomial series.

sections were similar to those for elastic scattering, with considerably larger statistical components (10% to > 30%) due to low intensities, less definition of scattered-neutron groups and to the necessity of the second-neutron-group source corrections.

The angle-integrated inelastic-scattering-cross-section results are summarized in Fig. 3. Excitations of the low-lying (370 to 555 keV), 2+, levels of the even palladium isotopes are prominent with the composite cross section exceeding 1 b at some energies. Generally, the observed cross sections are qualitatively consistent with the previously reported levels of the palladium isotopes.[1] Excitations of levels at energies of >2.0 MeV were repeatedly observed but the corresponding cross sections were uncertain and thus abandoned. The present inelastic-scattering results are reasonably consistent with the lower-energy values of Ref. 11 and the latter were used to extend the "eyeguides" of Fig. 3 to lower energies. The cummulative sum of these eyeguides is the total inelastic-scattering cross section to 2.0 MeV and it is in good agreement with the non-elastic cross section implied by the neutron total and elastic-scattering results of this work.

IV. INTERPRETATION AND DISCUSSION

The interpretation was based upon the conventional spherical optical model (OM).[13] Compound-nucleus (CN) contributions were calculated using the Hauser-Feshbach formula as modified by Moldauer.[14,15] All spherical calculations were carried out using the OM program ABAREX.[16] It was assumed that the elemental target could be reasonably represented by the even isotope ^{106}Pd as the even isotopes constitute $\approx$ 75% of the element and have similar level structure.[1] The effective target mass was taken to be 106.5 AMU. The calculations explicitly treated the excitation of the first 20 levels of ^{106}Pd extending up to 2.5 MeV using the level properties given in Ref. 1. Higher-energy excitations were approximated using the statistical parameters of Gilbert and Cameron.[17] The OM potential parameters were derived from the measured differential-elastic-scattering cross sections of Fig. 2 by concurrently fitting all of the measured values. In addition, several lower-energy neutron total-cross-section values were introduced at the time of fitting to assure a reasonable low-energy behavior. The present measurements span too narrow an energy range to reliably determine the energy dependences of the potential strengths. Thus, it was assumed that the real-potential energy dependence was -0.3 x E(MeV) in accord with commonly used global potentials.[18] The six OM parameters (real and imaginary strengths, radii and diffusenesses) were allowed to vary in the fitting procedures. There was no subsequent adjustment of the parameters derived from the fitting.

The resulting OM parameters are given in Table 2. They are qualitatively similar to those of a number of global parameter sets.[18] Quantitative and detailed discussion of the physical implications of these and other parameters obtained in similar analyses will be reported elsewhere.[19] The parameters of Table 2 provide an excellent description of the measured differential-elastic-scattering cross sections as illustrated in Fig. 4. They also provide a good description of the neutron total and angle-integrated elastic-scattering cross sections as illustrated in Fig. 1. The difference between measured and calcu-

Fig. 3   Observed Inelastic-Scattering Cross Sections of Elemental
         Palladium. The present experimental results are indicated by
         data symbols extended below 1.5 MeV using the values of Ref. 11.
         The light curves are "eyeguides" constructed through the measured
         values. The heavy curves are the result of model calculations as
         discussed in the text. Observed excitation energies ⌐re numerically
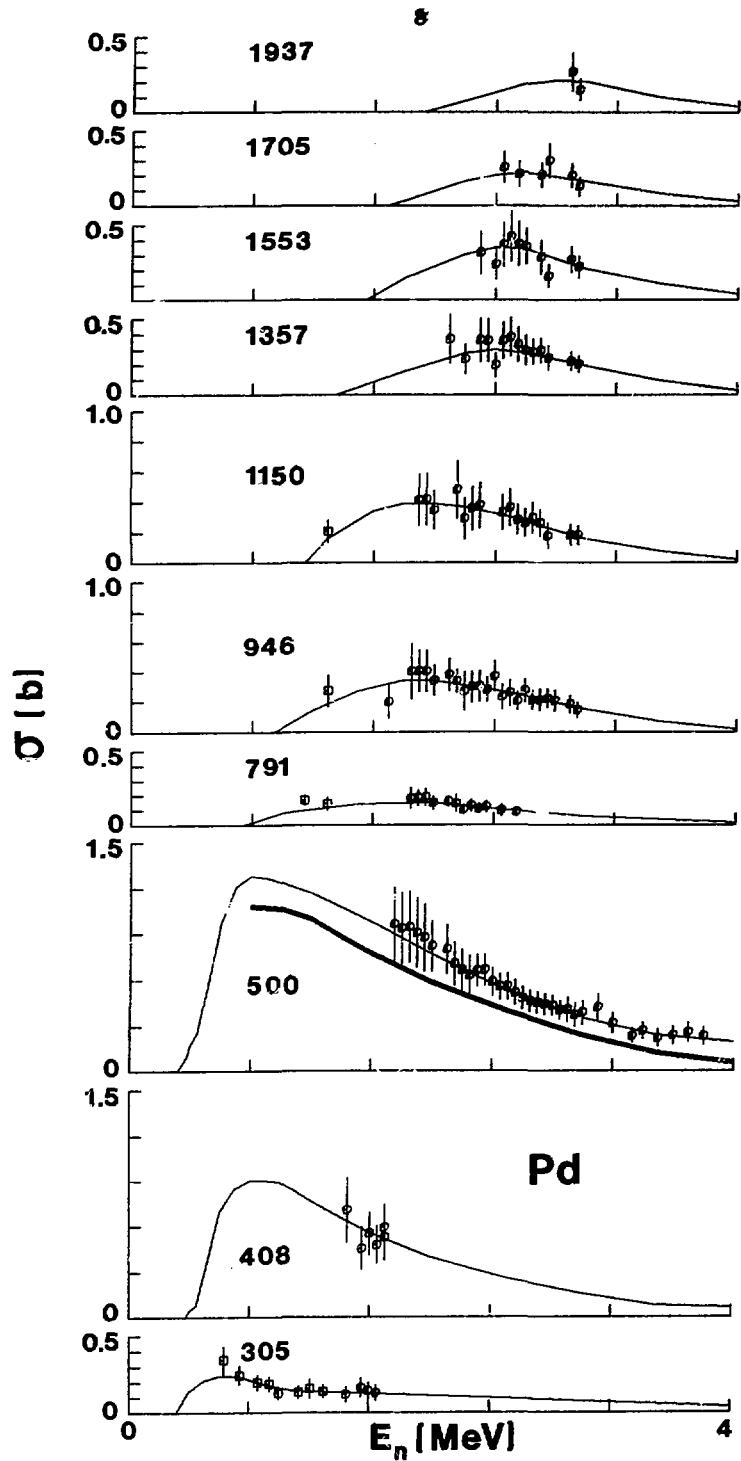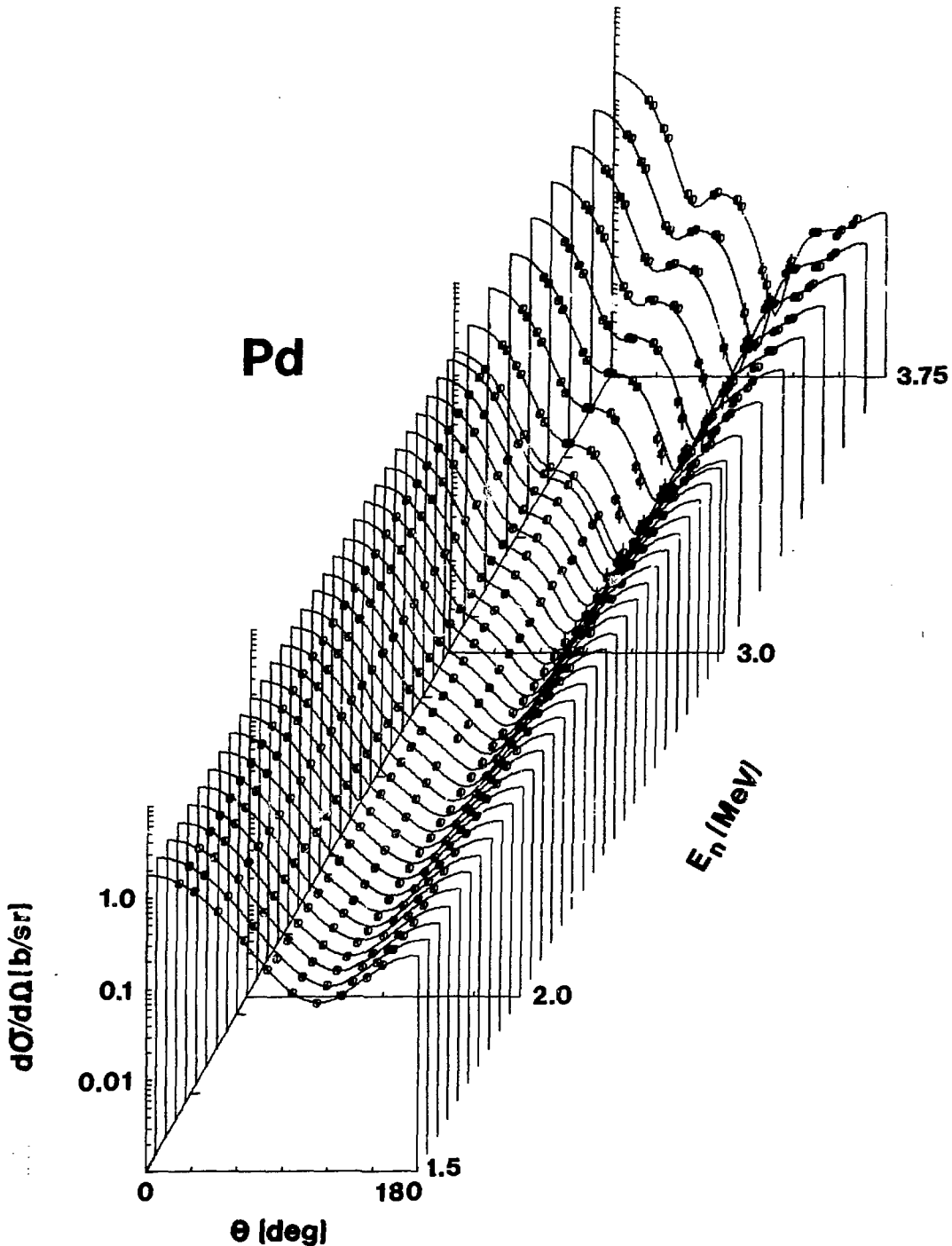   noted in keV.

Fig. 4 Measured and Calculated Differential-Elastic-Scattering Cross
Sections of Palladium. The present experimental results are
indicated by data symbols. The results of model calculations,
outlined in the text, are indicated by curves.

lated elastic-scattering cross sections at very low energies is due to the omission of the [105]Pd isotope in the calculations. However, there is some tendency for the calculated neutron total cross sections to be $\approx$ 100 mb lower than the measured values over much of the high-energy range. That is a 2.5% difference and little beyond the experimental uncertainty alone. Generally, comparisons of measured and calculated inelastic-scattering cross sections are difficult due to the uncertain level definition achieved in the measurements. However, the prominent excitations of the first 2+ levels of the even isotopes were calculated and supplemented with the calculated contributions from the odd [105]Pd isotope with the results shown in Fig. 3. These calculated results are $\approx$ 100 mb smaller than the measured values. This is not surprising as the even Pd isotopes are often cited as outstanding examples of vibrational nuclei and one could expect significant direct-vibrational excitation of their first 2+ levels not consistent with the spherical OM description outlined above. Indeed, assuming a perturbation approach based upon the parameters of Table 2, the direct-vibrational excitation was calculated using coupled-channels methods.[20] The direct component was $\approx$ 90 mb at 2.0 MeV and rose to $\approx$ 125 mb at 4.0 MeV. The addition of this direct component to the CN results brings the calculated total inelastic-scattering cross sections for the excitation of the 2+ levels into agreement with the measured values to within the experimental uncertainties. Concurrently, the neutron total cross section is increased by $\approx$ 100 mb over the higher-energy region resulting in nearly exact agreement with the measured values. The perturbation approach is, of course, an over simplification and a more rigorous interpretation should consider the influence of the direct process on the derivation of the OM parameters themselves. Such an exact procedure is extensive, costly and of uncertain benefit in the present elemental context and thus was not attempted. Its impact upon the OM parameters of Table 2 was estimated to be small.

V.   COMPARISONS WITH ENDF/B-V

The evaluated palladium data of ENDF/B-V[2] is presented on an isotopic basis. Therefore, the six isotopic components were combined, weighted on the basis of isotopic abundance, to obtain elemental evaluated values for comparison with the present experimental results. The evaluated and measured neutron total cross sections differ by small amounts at low energies ($\leq$ 0.5 MeV) but as the energy increases the ENDF/B values become progressively lower than the measured quantities by 8-10% as illustrated in Fig. 5 and Table 3. The ENDF/B elastic-scattering cross sections are universally larger than the measured values. The difference is a few percent at low energies and increases to 10-15% at 3 to 4 MeV as indicated in Fig. 5 and Table 3. The neutron total and elastic-scattering differences between measurement and evaluation are generally in opposite directions. Thus, there is a large difference between the non-elastic cross sections implied by the evaluation and the measurements; amounting to 30-50% (see Fig. 5 and Table 3). This difference is primarily associated with the inelastic scattering process as illustrated in Fig. 6. The elemental inelastic-scattering cross sections of the present measurements
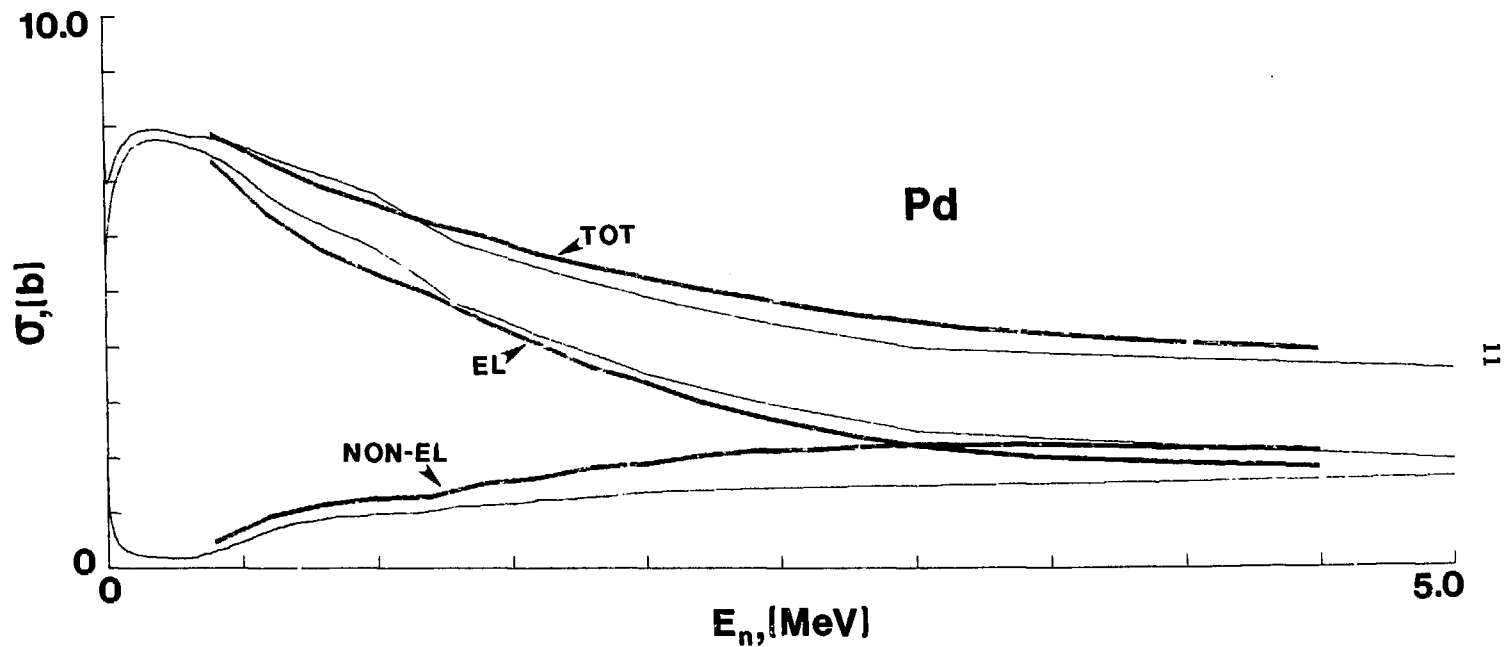
Fig. 5 Neutron Total, Elastic-Scattering and Non-Elastic Cross Sections
of Element Palladium. The heavy lines are "eyeguides" constructed
through the measured values. The light lines are the corre-
sponding cross sections taken from ENDF/B-V[2].
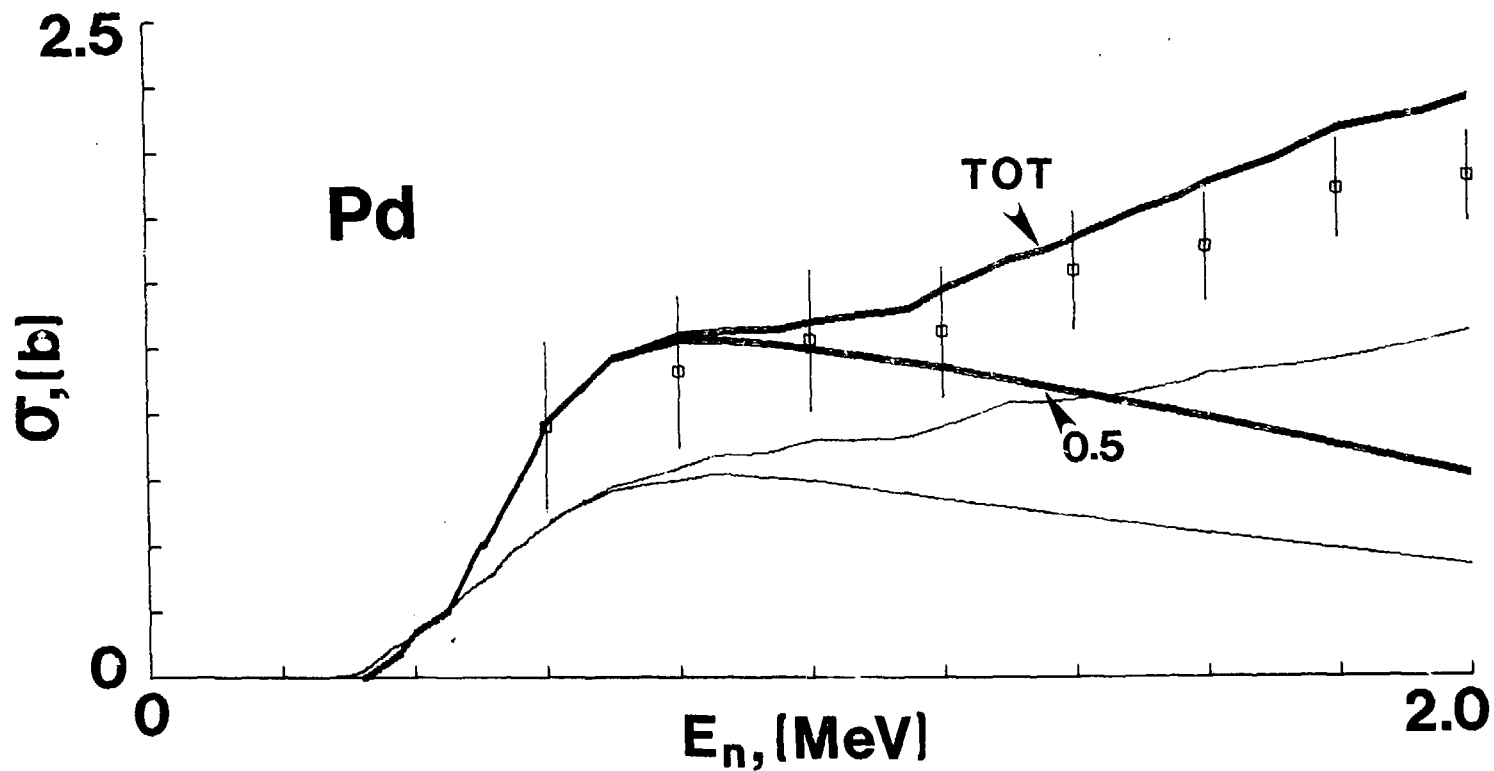
Fig. 6   Comparison of Measured and Evaluated Inelastic-Scattering Cross
          Sections of Elemental Palladium. The heavy curves indicate the
          total inelastic scattering cross sections and the cross sections
          for the excitations of all levels up to excitation energies of 580
          keV taken from the experimental measurements. The light curves
          represent the corresponding quantities taken from ENDF/B-V[2].
          The data symbols are representative non-elastic cross-section
          values implied by the present measurements.

imply a total inelastic-scattering cross section 40-60% larger than given by
the evaluated data files. That is a large difference much of which is
associated with the excitations of the first 2+ levels of the prominent
even isotopes. The inelastic-scattering differences are much larger than
the experimental uncertainties and there is reasonable consistency between
measured neutron total, elastic-scattering and inelastic-scattering cross
sections. The inelastic scattering cross sections are large and have
relatively low-energy thresholds. The above large discrepancies are
of applied significance as they considerably exceed the inelastic-cross-
section goals usually quoted for fission products.

VI. SUMMARY COMMENTS

The present measurements improve the experimental knowledge of neutron
total cross sections of elemental palladium from C.5 to 4.5 MeV, of elastic-
scattering cross sections from 1.5 to 3.8 MeV, and of the inelastic-scattering
cross sections corresponding to the excitation of levels to $\leq$ 2.0 MeV. The
experimental results form a good data base from which was deduced a spherical
optical potential that reasonably describes the observables. The resulting
parameters are similar to those of a general optical potential applicable to
this fission-product region.[19] Detailed comparisons of measured and calcu-
lated cross section suggests possible contributions from the direct-vibrational
excitations of the first-excited levels of the even palladium isotopes. The
experimental results were compared with the corresponding values given in
ENDF/B-V[2]. Large discrepancies between some measured and evaluated cross
sections were noted. In particular, measured and evaluated inelastic-
scattering cross sections differed by 40-60%. The latter discrepancy is
predominently attributed to the even isotopes of palladium. The total
inelastic-scattering cross section is large and has a relatively low-energy
threshold. Thus, large uncertainties in the inelastic-scattering cross sections
of these prominent fission products are of applied significance.

ACKNOWLEDGEMENTS

REFERENCES

1. Table of Isotopes, 7th Edition, C. M. Lederer and V. S. Shirley Eds., John Wiley and Sons, Inc., New York (1978).

2. Evaluated Nuclear Data File-B, Version-V, Brookhaven National Laboratory Report, ENDF-201 (1979), compiled by R. Kinsey.

3. D. Miller, Fast-Neutron Physics, Vol.-II, J. Marion and J. Fowler Eds., Interscience Pub., New York (1963).

4. A. Smith, R. Holt and J. Whalen, Argonne National Laboratory Report, ANL/NDM-43 (1978); see also Ref. 2.

5. W. Poenitz, J. Whalen and A. Smith, Nucl. Sci. and Eng., 78 333 (1981); also neutron total-cross-section data provided by W. Poenitz and J. Whalen, to be published.

6. A. Smith, P. Guenther, R. Larsen, C. Nelson, P. Walker and J. Whalen, Nucl. Instr. and Methods, 50 277 (1967).

7. A. Smith, P. Guenther and R. Sjoblom, Nucl. Instr. and Methods, 140 397 (1977).

8. A. B. Smith and P. T. Guenther, Argonne National Laboratory Report, ANL/NDM-63 (1982).

9. P. T. Guenther, "Elastic and Inelastic Neutron Scattering from the Even Isotopes of Tungsten", Univ. of Illinois Thesis (1977).

10. P. Guenther, A. Smith and J. Whalen, Phys. Rev., C12 1797 (1975).

11. A. Smith, P. Lambropoulas, P. Guenther and J. Whalen, Nucl. Sci. and Eng., 49 389 (1972). Data from this reference was averaged over ≈ 100 keV.

12. D. Foster and D. Glasgow, Phys. Rev., C3 576 (1971).

13. P. Hodgson, Nuclear Reactions and Nuclear Structure, Clarendon Press, Oxford (1971).

14. W. Hauser and H. Feshbach, Phys. Rev., 87 366 (1952).

15. P. A. Moldauer, Phys. Rev., C11 426 (1978); also private communications (1982).

16. P. Moldauer, "ABAREX, A Spherical Optical-Model Code," private communications (1982).

17. A. Gilbert and A. Cameron, Can. Jour. of Physics, 43 1446 (1965).

18. J. Rapaport, V. Kulkarni and R. Finley, Nucl. Phys., A330 15 (1979).

19. A. B. Smith, to be published.

20. P. Moldauer, "JUPREX, A Coupled-Channels Model Code," private communications (1982).

Table 1
Observed Inelastic-Neutron Excitation Energies

No.	E_x(MeV)[a]	Contributing Isotopes[b]
1.	0.305 ± 0.025	105
2.	0.408 ± 0.052	105, 108 and 110
3.	0.5[c]	All
4.	(0.642)[d]	105
5.	0.791 ± 0.026	105
6.	0.946 ± 0.024	105, 108 and 110
7.	1.150 ± 0.031	105, 106 and 108
8.	1.357 ± 0.054	104, 105, 108 and 110
9.	1.553 ± 0.054	105, 106, 108 and 110
10.	1.705 ± 0.069	All
11.	1.937 ± 0.048	All
12.	(2.059)[d]	---
13.	(2.110)[d]	---
14.	(2.207)[d]	---

a. Uncertainty defined as RMS deviation from the simple average of a number of observations and does not necessarily reflect scattered-neutron resolutions.

b. Estimates based upon level structures as given in Ref. 1, the 1%-abundant ^{102}Pd is ignored.

c. Inclusive of all excitations up to 580 keV.

d. Values based upon limited observation precluding quantitative uncertainty estimate.

Table 2

Optical-Model Parameters for Palladium

Real Potential[a]

Strength V = 47.348	MeV
Radius[b] r_o = 1.260	F
Diffuseness a_V = 0.636	F
$V \times r_o^2$ = 75.17	MeV $\times$ F^2
J/A^c = 441.18	MeV $\times$ F^3

Imaginary Potential[d]

Strength W = 10.16	MeV
Radius r_o = 1.231	F
Diffuseness a_W = 0.527	F
$W \times A_W$ = 5.36	MeV $\times$ F
J/A^c = 88.36	MeV $\times$ F^3

a. Saxon form; assumed energy dependence of
   $-0.3 \times E(MeV)$; throughout, spin-orbit potential
   of Thomas form with a 6 MeV strength.

b. All radii expressed as $R = r_o \times A^{1/3}$.

c. Potential integral per nucleon.

d. Saxon-derivative form.

Table 3

Comparison of Present
Experimental Results with ENDF/B-V[2] Values

E_n(MeV)	$\delta\sigma_t$	$\delta\sigma_{el}$	$\delta \equiv (\frac{EXP - ENDF}{ENDF})$ $\delta\sigma_{non-el}$	$\delta\sigma_{inel}$
0.5	−0.6%	−1.3%	+43.0%	+42.0%
1.0	−2.7%	−8.2%	+27.0%	+50.0%
1.5	+4.1%	−3.8%	+34.0%	+63.0%
2.0	+7.3%	−4.3%	+35.0%	+67.0%
2.5	+10.0%	−8.5%	+44.0%	−−
3.0	+11.5%	−11.6%	+48.0%	−−
3.5	+8.4%	−14.9%	+44.0%	−−
4.0	+6.9%	−12.0%	+35.0%	−−